DOI: https://doi.org/10.24425/amm.2025.155494

T.T. $TRUC_{\bullet}^{1,2}$, H.N. $MINH_{\bullet}^{1,2*}$, M.D. $PHU_{\bullet}^{1,2}$, L.H. $HUY_{\bullet}^{1,2}$, D.Q. $MINH_{\bullet}^{1,2}$

STUDY GEOPOLYMER FROM DREDGED SEDIMENT, FLY ASH, AND CAUSTIC SODA USING THE TAGUCHI EXPERIMENTAL PLANNING METHOD

In this study, the Taguchi experimental planning method was employed to evaluate the influence of three factors – dredged sediment content (30-70 wt.%), waste ceramic wool content (3-7 wt.%), and NaOH concentration in the alkaline activator solution (8-14 M) – on the compressive strength of geopolymer mortar prepared with sea sand, brine, and hydrothermal curing. The results indicated that lower sediment content and moderate levels of ceramic wool and NaOH concentration within the investigated ranges enhanced compressive strength. A regression model was developed to predict compressive strength, demonstrating good agreement with experimental values. Based on the model, the maximum allowable dredged sediment content to achieve compressive strengths of 3.5 MPa and 20 MPa – corresponding to low- and high-strength grades according to the Vietnam national standard TCVN 6477:2016 for concrete bricks – was found to be 70 wt.% and 39 wt.%, respectively. This approach presents a promising solution for the sustainable treatment of dredged sediment while meeting construction performance requirements.

Keywords: Taguchi method; fly ash; geopolymer mortar; sustainable treatment of dredged sediment; sea sand and brine

1. Introduction

In ports, dredging activities are becoming increasingly common, resulting in a significant amount of waste dredged sediment (DS) that requires treatment. Various methods can be applied to handle the DS, including burial, sinking, recycling, and reuse. While landfill and sinking methods are commonly employed, they lack long-term economic and environmental sustainability [1]. Despite extensive research on recycling techniques for DS, only a minor fraction, approximately 10%, is recycled and reused today [2].

Ordinary Portland cement (OPC) is commonly used as a binder to solidify DS [3,4]. However, the OPC is a significant source of CO₂ emissions (around 1 kg of CO₂ per 1 kg of OPC) [5]. Solidifying DS through geopolymerization has become an increasingly attractive research trend [6,7]. Geopolymerization emits considerably less CO₂ than cement production and utilizes waste materials such as fly ash (FA) and slag as raw materials [8,9]. The geopolymerization process involves a reaction of aluminosilicate and an alkaline activator solution (AAS), forming a three-dimensional network of Si-O-Al-O bonds [10]. Using statistical modeling is a popular approach in recent materials studies because it allows for quick and efficient evaluation of multiple influencing factors with fewer experiments required [4,11-13].

The geopolymer materials may possess qualities equivalent to or even better than OPC concrete [14]. Geopolymer concrete has significantly better resistance to seawater ions such as Cl and SO_4^{2-} than OPC concrete [15-18]. These ions are always present in DS taken from seaports. This advantage demonstrates the sustainability of using the geopolymerization method for DS treatment. Likewise, it is also feasible to incorporate sea sand and seawater into this process, which is particularly beneficial given the current shortage of river sand and fresh water in coastal regions. Previous studies that employed sea sand and seawater in GPC reported no harmful impact from Cl⁻ and SO_4^{2-} ions on the strength of this material [19].

In addition to DS, the waste ceramic wool (WCW) removed from discarded ceramic fiber boards in furnaces is a solid waste requiring proper disposal. Due to its SiO₂ and Al₂O₃ content, WCW can serve as both a filler material and a reactive component in geopolymerization. Furthermore, adding fibrous WCW to geopolymer mortar can improve mechanical strengths and the thermal resistance of GPC [20,21]. Besides composition, curing conditions also play an important role in determining GPC performance. Typically, GPC is cured at temperatures ranging from 40-90°C to accelerate the geopolymerization process, thus enhancing compressive strength [22]. According to Davidovits,

^{*} Corresponding author: hnminh@hcmut.edu.vn



HO CHI MINH CITY UNIVERSITY OF TECHNOLOGY (HCMUT), FACULTY OF MATERIALS TECHNOLOGY, DEPARTMENT OF SILICATE MATERIALS, 268 LY THUONG KIET STREET,

² VIETNAM NATIONAL UNIVERSITY HO CHI MINH CITY, LINH TRUNG WARD, THU DUC CITY, HO CHI MINH CITY, VIETNAM

the empirical chemical formula for geopolymers is represented as $M_n\{(SiO_2)_zAlO_2\}_n \cdot wH_2O$, where M denotes a cation, n indicates the degree of polycondensation, w represents the number of water molecules, and z equals 1, 2, or 3 [23]. Curing under hydrothermal conditions has been shown to enhance the formation of geopolymers. This method significantly shortens processing time, allowing geopolymers to gain strength at an earlier age [24]. Additionally, hydrothermal curing promotes the formation of more Si(Q⁴) structures than dry curing [25]. These structures help immobilize sodium ions (Na⁺), prevent alkali leaching, and stabilize heavy metals by forming insoluble metal-silicate compounds, such as Pb₃SiO₅ [26]. Hydrothermally cured geopolymer samples showed compressive strength over twice that of dry-cured samples. They also exhibited no signs of the white hair phenomenon on the sample surface, indicating minimal carbonation when exposed to air [27].

In this study, the simultaneous influence of composition factors, including DS, WCW, and NaOH concentration (CM_{NaOH}) of AAS on the 7-day compressive strength of geopolymer mortar (hydrothermal curing at 180°C for 13.5 hours followed by curing in an air environment) was investigated using the Taguchi planning method. The regression equation was solved to achieve a minimum compressive strength of 3.5 MPa in accordance with national standard TCVN 6477:2016 for concrete bricks while maximizing the DS content. X-ray Diffraction (XRD) analysis was also conducted to examine the formation of the geopolymer structure. This approach provides a practical solution for the large-scale use of DS in the production of geopolymer mortar, thereby contributing to sustainable construction practices.

2. Materials and methods

2.1. Materials

The raw materials were FA, DS, WCW, and sea sand. The FA was sourced from Duyen Hai 1 Thermal Power Plant, Tra Vinh Province, Vietnam. DS was collected from dredging at Long An International Port, Long An Province, Vietnam. WCW was waste from ceramic kiln insulation panels and was chopped in a blender for 1 min to form homogeneous pieces. Sand from Hoi An Beach, Duc Pho Town, Quang Ngai Province, Vietnam, has a fineness modulus of 2.05 and a density of 2.52 g/cm³. The AAS was prepared from sodium hydroxide (NaOH) flakes and brine. The brine salinity was set at 35‰, simulating the highest salinity recorded in Vietnam's seawater.

2.2. Methodology

2.2.1. The Experimental Procedure

The compressive strength of geopolymer mortar (denoted as y) depends on many technological variables, such as raw material composition, forming process, and curing conditions

(time, temperature, humidity, environment). In this study, three variables were investigated, which are the content (wt.%) of DS (denoted as x_1), the content (wt.%) of WCW (denoted x_2), and CM_{NaOH} of AAS (M) (x_3). Other parameters were kept constant during the experiment. The hydrothermal method in an autoclave at 180° C for 13.5 hours was chosen to cure geopolymer mortar because it ensures strength development at the age of 7 days.

The ranges of variables x_1 , x_2 , and x_3 were selected to ensure the ability to shape samples using the pouring method into $4 \times 4 \times 16$ (cm) steel molds. With the same water content, when $x_1 > 70\%$, the mortar mixture became too stiff to mold, and when $x_1 < 30\%$, it became overly fluid. Similarly, the WCW content was selected within the range of 3-7%. According to previous experiments [22], the CM_{NaOH} of AAS was set between 8-14 M. Thus, the compressive strength of geopolymer mortar (y) can be expressed as Eq. (1):

$$y = f(x_1, x_2, x_3) \tag{1}$$

where: $30 \le x_1 \le 70$; $3 \le x_2 \le 7$; $8 \le x_3 \le 14$.

The experimental flow chart illustrating the sequence of procedures is presented in Fig. 1.

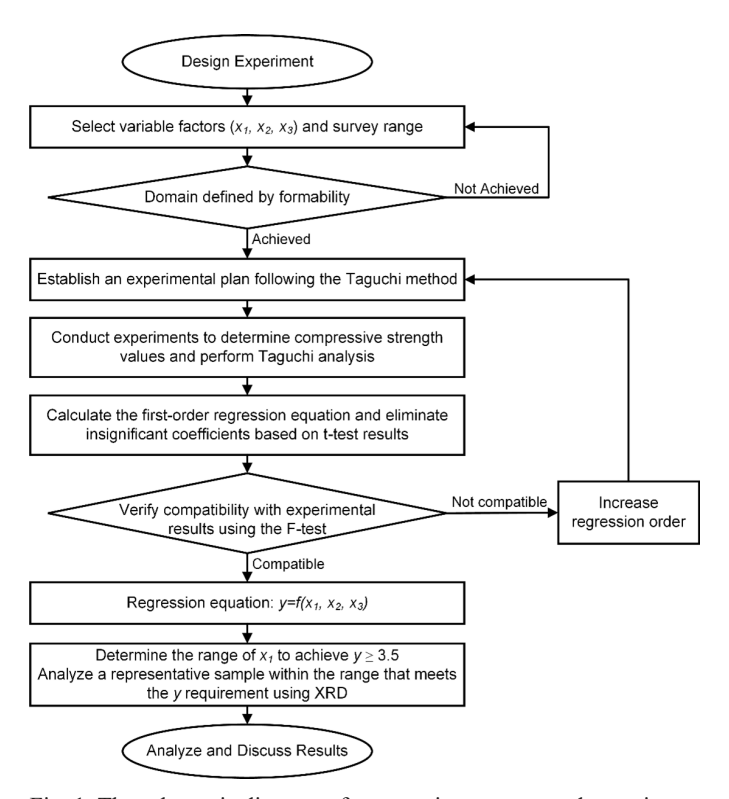


Fig. 1. The schematic diagram of prototyping process and experimentation

2.2.2. Taguchi's Experimental Plan

The experiments were conducted according to the Taguchi L9 orthogonal array, as shown in TABLE 1. Since the factors have different magnitudes and measurement units, the values of the variables were encoded as [-1, 0, 1] to ensure consistency in the regression analysis. The coefficients of the regression

	Mix ID	Total solid powder content (g)	Water content (g)	Sea sand content (g)	DS (%)	WCW (%)	CM _{NaOH} (M)
	1	900	300	500	30	3	8
	2	900	300	500	30	5	11
	3	900	300	500	30	7	14
Taguchi L9	4	900	300	500	50	3	11
orthogonal	5	900	300	500	50	5	14
array	6	900	300	500	50	7	8
	7	900	300	500	70	3	14
	8	900	300	500	70	5	8
	9	900	300	500	70	7	11
Center-point experiments	10	900	300	500	50	5	11
	11	900	300	500	50	5	11
	10	000	200	500	50	-	1.1

Mix design according to the Taguchi L9

equation were determined using the least squares method. Additionally, three center-point experiments (50% DS, 5% WCW, 11 M CM_{NaOH} of AAS) were performed to assess reproducibility variance. This value was used to evaluate the statistical significance of the regression coefficients using the t-test and the compatibility of the regression equation using the F-test. If the first-order regression equation is incompatible based on the F-test, two out of three center-point experiments (Mix ID 10-11) will be incorporated, in addition to the nine experiments from the Taguchi L9 array, to develop a second-order regression equation.

The sample preparation procedure followed: First, FA and DS were mixed in a mixer for 1 minute. Then, AAS was poured in and stirred for 2 minutes. Sea sand was added slowly over 30 seconds while continuously mixing. WCW was added in the next 30 seconds. The mixing time was 5 min, starting from the moment the sand was added.

The mixed mortar was poured into $4\times4\times16$ (cm) steel molds. After 24 hours, the samples were de-molded and hydrothermally cured in an autoclave at approximately 180° C for 13.5 hours. The samples were cured at room temperature until they reached 7 days of age for compressive strength determination (R_C). After 7 days of curing (including hydrothermal and subsequent air curing), the material samples were evaluated for compressive strength using a Phoenix Pisces 300/30 kN machine. Representative samples (meeting $R_C \ge 3.5$ MPa) were analyzed by XRD to clarify the microstructural changes.

The Taguchi method uses the signal-to-noise ratio (S/N) calculated from the loss function to evaluate the impact trend of factors on the output results. In this study, the 'larger-isbetter' formula was used to calculate the S/N ratio as shown in Eq. (2) [28]:

$$\frac{S}{N} = -10\log_{10}\left(\frac{1}{n}\sum_{i=1}^{n}\frac{1}{y_i^2}\right)$$
 (2)

Where n is the number of repeated experiments, s is the standard deviation, and y_i is the average 7-day compressive strength of the sample in experiment i.

2.2.3. Analysis of the Regression Equation

Based on the regression equation obtained, determine the maximum DS content for the material to have a compressive strength greater than 3.5 MPa, the minimum compressive strength required for concrete bricks according to Vietnam national standard TCVN 6477:2016 [29].

3. Results and discussion

3.1. The Impact of Various Factors on Compressive Strength

The 7-day compressive strength results of the samples with the S/N ratio calculated according to the "larger the better" formula are presented in TABLE 2.

TABLE 2
The signal-to-noise (S/N) ratio for compressive strength evaluation

Mix	Variables			Enco	ded var		S/N		
ID	DS (%)	WCW (%)	CM _{NaOH} (M)	X_1	<i>X</i> ₂	X_3	y (MPa)	ratio	
1	30	3	8	-1	-1	-1	15.20	23.64	
2	30	5	11	-1	0	0	26.63	28.51	
3	30	7	14	-1	1	1	16.71	24.46	
4	50	3	11	0	-1	0	10.71	20.60	
5	50	5	14	0	0	1	10.85	20.71	
6	50	7	8	0	1	-1	9.73	19.76	
7	70	3	14	1	-1	1	5.60	14.96	
8	70	5	8	1	0	-1	4.67	13.39	
9	70	7	11	1	1	0	4.74	13.52	

After processing the S/N ratios using basic standard Taguchi formulas, the results in TABLE 3 revealed that the DS content had the most significant impact on the compressive strength of the material samples, followed by the CM_{NaOH} of AAS, and lastly, the WCW content used.

The impact of factor levels on compressive strength							
Variables		x_1	x_2	x_3			
	Level 1	25.53	19.73	18.93			

TABLE 3

Vari	ables	x_1	x_2	x_3	
	Level 1	25.53	19.73	18.93	
S/N ratios	Level 2	20.36	20.87	20.87	
	Level 3	13.96	19.25	20.04	
Mean (m)		19.95	19.95	19.95	
M	ax	25.53	20.87	20.87	
Max	. – m	5.59	0.92	0.92	
%Influe	ence (ε_i)	75.19	12.37	12.44	
Ra	ınk	1	3	2	

The S/N ratio at the examined levels of the factor variables is shown in Fig. 2. The trend for increasing the compressive strength of the sample involved a decrease in the DS content used, alongside a moderate level use of WCW (5%) content and CM_{NaOH} of AAS (11 M). A regression equation was established to more clearly determine the minimum DS reduction range required to achieve the necessary compressive strength.

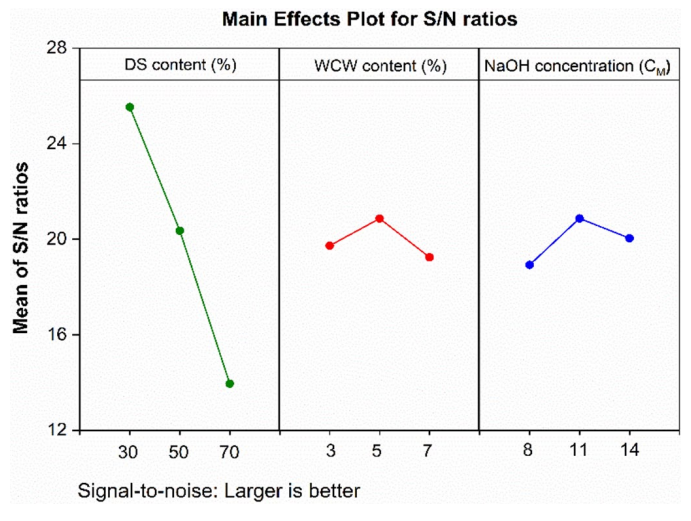


Fig. 2. Mean signal-to-noise (S/N) ratios for compressive strength

3.2. Analyze Regression Equation

After conducting first-order regression using the initial nine experiments, the F-test indicated that the regression equation was incompatible with the experimental data. Consequently, a quadratic regression analysis was conducted using 11 experiments (initial nine experiments and two center-point experiments with average compressive strengths of 14.19 MPa and 13.65 MPa). By removing insignificant coefficients from the encoded variable equation, the second-order regression equation was determined to be compatible with the experimental data through the F-test. The final quadratic regression equation is presented in Eq. (3).

$$y = -43.954 - 1.364x_1 + 15.233x_2 + 11.859x_3 +$$

$$+ 0.00911x_1^2 - 0.859x_2^2 - 0.402x_3^2 - 0.605x_2x_3$$
 (3)

TABLE 4 displays the compressive strengths of three samples with randomly selected component values. In these cases, the comparison between the calculated ($y_{predicted}$) and actual (y_{actual}) values indicates that the actual compressive strengths were consistently higher than those predicted by the regression equation. This suggests that the model may provide conservative estimates, which could offer a safety margin for practical applications.

TABLE 4
Deviation analysis between predicted and actual compressive strength values

Test	DS (%)	WCW (%)	CM _{NaOH} (M)	Ypredict	Yactual
1	39	6	13	16.22	18.19
2	60	4	9	6.58	8.69
3	45	5	10	15.94	16.96

Regression Eq. (3) shows the relationship of DS, WCW, and CM_{NaOH} of AAS within the range $(30 \le x_1 \le 70; 3 \le x_2 \le 7; 8 \le x_3 \le 14)$ to the compressive strength as a quadratic function. Some response surfaces from this regression equation are shown in Fig. 3 using the OpenCV-Python tool. Fig. 3a illustrates the graph of Eq. (3) with $x_3 = 11$, Fig. 3b represents the graph of Eq. (3) when $x_2 = 5$, and Fig. 3c corresponds to $x_1 = 50$.

The diagrams in Fig. 3a and Fig. 3b show that the compressive strength (y) increases as the DS content decreases within the investigated region. However, in Fig. 3c, compressive strength reaches its maximum at 50% DS, aligning with the previous S/N ratio analysis of factor effects. In Fig. 3d, the variables are represented on three axes (Ox, Oy, Oz), and the compressive strength (y) is depicted on colored curved surfaces in 3D space. On the limiting surface $x_1 = 30$ (30% DS), the curved surfaces form concentric circles centered at $x_2 = 5$, $x_3 = 11$ (5% WCW, 11 M CM_{NaOH} of AAS – indicating the maximum y values.

Due to the lack of alkali activity, DS acts primarily as a filler, reducing the strength of geopolymer materials [30,31]. In contrast, FA is the principal reactive component that significantly contributes to compressive strength development in the DS-FA geopolymer system [32]. However, for DS treatment, it is convenient to choose the highest DS content while still achieving the desired strength by solving the regression equation.

For example, to meet the minimum brick grade of $y \ge 3.5$ MPa (TCVN 6477:2016), with $x_2 = 5$ and $x_3 = 11$, the expansions are expressed in Eq. (4) and Eq. (5) as follows:

$$\Rightarrow y = 59.328 + 0.00911x_1^2 - 1.364x_1 \ge 3.5 \tag{4}$$

$$\Rightarrow y = (x_1 - 74.86)^2 + 522.7304 \ge 0$$
 (5)

 \Rightarrow True for all x_1 in the investigated range.

In the investigated range, the compressive strength met the requirement $y \ge 3.5$ MPa requirement for all variable values. Therefore, up to 70% DS, representing the experimental threshold where the mixture remains shapeable, can produce

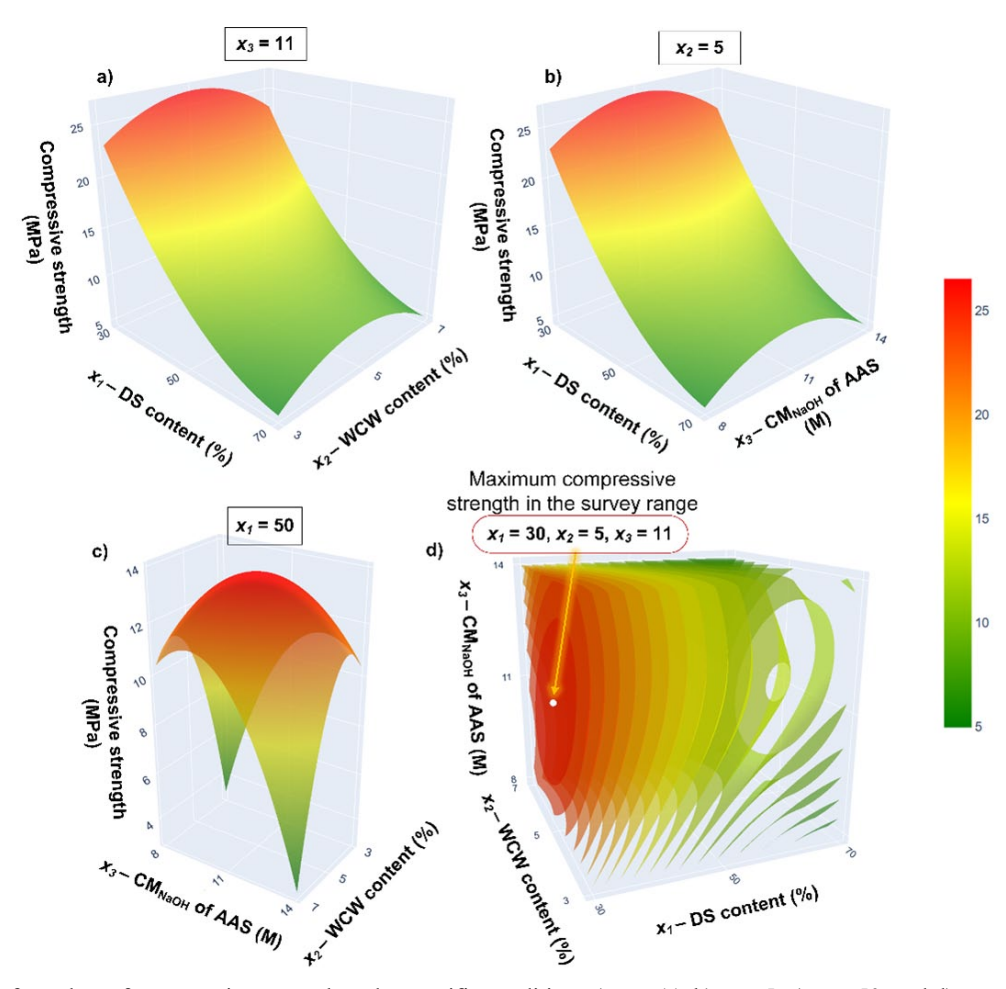


Fig. 3. Response surface plots of compressive strength under specific condition: a) $x_3 = 11$, b) $x_2 = 5$, c) $x_1 = 50$, and d) no variables are fixed

geopolymer mortar that meets the minimum strength requirement for the lowest grade of concrete bricks (3.5 MPa).

When increasing the required compressive strength to higher concrete brick grades (5-20 MPa), solving the regression equation provides the maximum allowable DS content, as shown in TABLE 5. For the highest grade in the standard, the permissible DS content was reduced to 39%.

TABLE 5 Maximum allowable DS content (x_1) corresponding to different minimum compressive strength (y) levels

y (MPa)	3.5	5	7.5	10	12.5	15	20
Minimum x_1 (%)	All	All	All	61.1	53.3	47.7	39.0

3.3. X-Ray Diffraction Analysis

The XRD pattern of a representative sample that meets the minimum compressive strength requirement of 3.5 MPa within the investigated range (50% DS, 5% WCW, 11 M $\rm CM_{NaOH}$ of AAS) is shown in Fig. 4. In the raw material, the main mineral components of FA were quartz and mullite. In comparison, the main mineral components of DS were quartz, calcite, and muscovite. In contrast to FA and DS, WCW only exhibited a broad

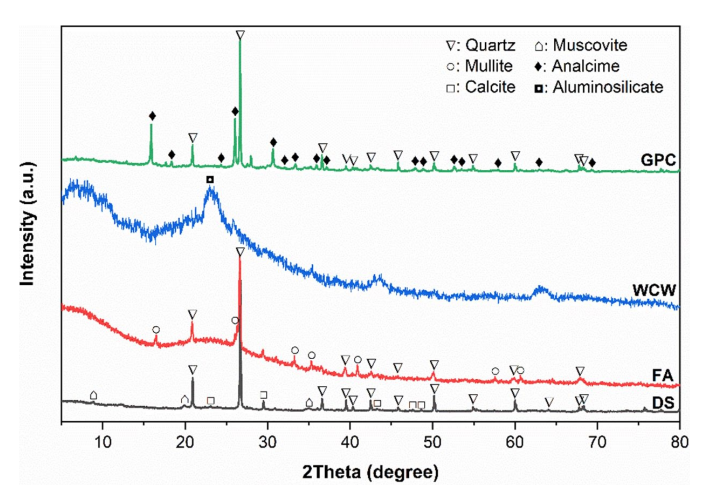


Fig. 4. The XRD patterns of geopolymer mortar sample (50% DS, 5% WCW, 11 M $\rm CM_{NaOH}$ of AAS, at 7 days) and raw materials (FA, DS, WCW)

band characteristic of aluminosilicate. The limited amorphous phase in DS reduced its reactivity in the geopolymerization process, which explains the previously observed low dissolution of Si and Al from DS in NaOH solution. The XRD results of geopolymer mortar depicted a semi-crystalline structure with the main crystalline components including quartz and analcime

 $(Na_{0.9}(Al_{0.9}Si_2)O_6)(H_2O)$, ICDD 01-076-6569) – minerals characteristic of geopolymer materials. Some minerals in the raw materials, such as calcite, mullite, and muscovite, were barely detectable in the final geopolymer mortar, suggesting their participation in the geopolymerization process. This transformation confirmed the occurrence of geopolymerization, which involved the dissolution of AS material and the generation of gel. Subsequently, the gel partially transformed into zeolite crystals, resulting in the formation of the mineral analcime.

4. Conclusions

The Taguchi method was used to analyze the effects of factors on the compressive strength of geopolymer mortar. Among the variables, dredged sediment (DS) content had the most significant influence, followed by the concentration of NaOH in the alkaline activator solution (CM_{NaOH} of AAS) and waste ceramic wool (WCW) content. An increase in DS content led to a reduction in compressive strength. Regression analysis identified an optimal mixture containing 5 wt.% WCW and 11 M CMNaOH of AAS, which could accommodate up to 70 wt.% DS while maintaining a compressive strength of at least 3.5 MPa, or 39 wt.% DS to achieve 20 MPa. XRD analysis identified analcime as the characteristic geopolymer mineral, indicating the formation of a semi-crystalline structure in hydrothermally treated samples. The regression equation enabled the estimation of component proportions in the DS treatment across various scales. The experimental results showed good agreement with the predicted values, supporting the applicability of the regression equation for estimating the compressive strength of geopolymer materials in specific applications.

Acknowledgments

This research is funded by Vietnam National University Ho Chi Minh City under grant number B2024-20-27. We acknowledge Ho Chi Minh City University of Technology (HCMUT), VNU-HCM for supporting this study.

REFERENCES

- [1] C.N. Mulligan, R.N. Yong, B.F. Gibbs, Journal of Hazardous Materials **85**, 1-2 (2001).
- [2] S. Lirer, B. Liguori, I. Capasso, A. Flora, D. Caputo, Journal of Environmental Management 191, (2017).
- [3] H. Wang, R. Zentar, F. Ouendi, Academic Journal of Civil Engineering **39**, 1 (2021).
- [4] T.D. Thai, N.M. Huynh, T. Luu, K. Kieu Do Trung, N. Nguyen Vu Uyen, M. Do Quang, Vietnam Journal of Science and Technology **62**, (2024).
- [5] M.F. Nurruddin, S. Haruna, B.S. Mohammed, I.G. Sha'aban, International Journal of Advanced and Applied Sciences 5, 1 (2018).

- [6] A. Alloul, High-Performance Geopolymer and Low-Carbon Cementitious Binders Using Flash-Calcined Dredged Sediments and Excavated Clays, University of Lille, 2024.
- [7] E. Mahfoud, K. Ndiaye, W. Maherzi, S. Aggoun, M. Benzerzour, N.E. Abriak, Developments in the Built Environment **16**, (2023).
- [8] W.W.A. Zailani, N.M. Apandi, M.M.A. Abdullah, M.F.M. Tahir, I.N. Sinarta, N.K.A. Agustini, S. Abdullah, Archives of Metallurgy and Materials 69, 1 (2024).
- [9] L. Jia-Ni, L. Yun-Ming, M.M.A.B. Abdullah, T. Hoe-Woon, H. Yong-Jie, O. Shee-Ween, O. Wan-En, Archives of Metallurgy and Materials 69, 4 (2024).
- [10] S. Sharma, M.E. Scholar, International Journal of Computational Engineering Research **12**, 12 (2015).
- [11] T.D. Thai, N.M. Huynh, D.T.K. Kieu, V.U.N. Nguyen, Q.M. Do, International Journal of Engineering Transactions C: Aspects 38, 3 (2025).
- [12] S. Karthik, K.S.R. Mohan, Crystals 11, 11 (2021).
- [13] S.V. Dave, A. Bhogayata, Construction and Building Materials **262**, (2020).
- [14] M. Varuthaiya, C. Palanisamy, V. Sivakumar, G. Pushpanathan, Journal of Ceramic Processing Research 23, 6 (2022).
- [15] G.C. Reddy, K.H.K. Reddy, Earth Environ. Sci. (2023).
- [16] B. Zhang, Sustainable Materials and Technologies 40, (2024).
- [17] F. Hannanee Ahmad Zaidi, R. Ahmad, M. Mustafa Al Bakri Abdullah, M. Faheem Mohd Tahir, Z. Yahya, W. Mastura Wan Ibrahim, A. Syauqi Sauffi, Materials Science and Engineering 551, 1 (2019).
- [18] W. Li, E.D. Shumuye, T. Shiying, Z. Wang, K. Zerfu, Case Studies in Construction Materials **16**, (2022).
- [19] N. Van Dong, N.T. Trung, P.T. Tung, International Journal of Geomate. 23, 99 (2022).
- [20] A. Dalğıç, B. Yılmazer Polat, Applied Sciences 14, 4 (2024).
- [21] D.Q. Minh, N.V. Uyen Nhi, N. Hoc Thang, Journal of Polymer & Composite 8, 2 (2020).
- [22] Z. Moujoud, S. Sair, H. Ait Ousaleh, I. Ayouch, A. El Bouari, O. Tanane, Construction and Building Materials 388, (2023).
- [23] J. Davidovits, Geopolymer Chemistry and Applications, France 2020
- [24] R. Abd Razak, S.N.S.S. Izman, M.M. Al Bakri Abdullah, Z. Yahya, A. Abdullah, R. Mohamed, Archives of Metallurgy and Materials 68, 2 (2022).
- [25] N.H. Thang, B.K. Thach, D.Q. Minh, International Journal of Technology 12, 4 (2021).
- [26] M. Ramadan, A.O. Habib, M.M. Hazem, M.S. Amin, A. Mohsen, Construction and Building Materials **367**, (2023).
- [27] T.T. Truc, H.N. Minh, D.Q. Minh, Ceramics-Silikáty 69, 1 (2025).
- [28] A. Mitra, Wiley Interdisciplinary Reviews: Computational Statistic **3**, 5 (2011).
- [29] https://isoq.vn/van-ban-phap-quy/tcvn-6477-2016-gach-be-tong/.
- [30] K. Komnitsas, Journal of Environmental Chemical Engineering. 4, 4 (2016).
- [31] S. Hosseini, N.A. Brake, M. Nikookar, Ö. Günaydın-Şen, H.A. Snyder, Construction and Building Materials **301**, (2021).
- [32] M. Brahim, K. Ndiaye, S. Aggoun, W. Maherzi, Buildings 12, 4 (2022).